Investigation of the Substituting Effect of Chromium on the Electronic Structures and the Half-Metallic Ferromagnetic Properties of BaO

Habiba Lakhdari, Bendouma Doumi, Allel Mokaddem, Adlane Sayede, João Pedro Araújo, Abdelkader Tadjer, Mohammed Elkeurti

Investigation of the Substituting Effect of Chromium on the Electronic Structures and the Half-Metallic Ferromagnetic Properties of BaO

Habiba Lakhdari[1] · Bendouma Doumi[2] · Allel Mokaddem[3,4] · Adlane Sayede[5] · João Pedro Araújo[6] · Abdelkader Tadjer[7] · Mohammed Elkeurti[1]

Abstract

The first-principle methods of density functional theory were used to investigate the doping effect of 3d chromium (Cr) impurities on the electronic properties and the ferromagnetic arrangement of (BaO) barium oxide such as $Ba_{1-x}Cr_xO$ compounds at concentrations $x = 0.25$, 0.5, and 0.75. The p–d exchange coupling between 2p states of oxygen (O) and 3d (Cr) partially filled levels induces magnetism in the $Ba_{1-x}Cr_xO$ compounds. The majority- and minority-spin states exhibit respectively metallic and semiconducting features, leading to a half-metallic (HM) character with 100% spin polarization for all concentrations. The $Ba_{0.75}Cr_{0.25}O$, $Ba_{0.5}Cr_{0.5}O$, and $Ba_{0.25}Cr_{0.75}O$ compounds have integral total magnetic moments of 4 μ_B per Cr atom with HM gaps of 0.055, 0.218, and 0.308 eV, respectively. These behaviors form accurate half-metallic ferromagnets and make $Ba_{1-x}Cr_xO$ as potential materials for possible spintronics applications.

Keywords DFT · Half-metallic ferromagnets · p–d exchange interaction · Cr-substituted BaO

1 Introduction

In recent years, the diluted magnetic semiconductors (DMS) have attracted significant interest because they are a one class of half-metallic ferromagnets (HMFs) owing to their electronic structures that exhibit semiconducting character in onespin channel and metallic nature in the other direction, which make them promising materials for spin injection in spintronics [1–7] The HMFs can be extensively used in spintronics devices as spin injection, spin filters, spin valves, tunnel junctions and magneto-resistive randomaccess memory [8] Spintronics devices have many advantages over conventional semiconductor devices such as non-volatility, increased transistor density, lower electric power consumption and higher dataprocessing speed [9–11].

The DMS based on transition metal-doped II–VI semiconductors are promising candidates for spintronics applications because of their half-metallic ferromagnetic performance [12–14] and they show the stability of ferromagnetic state at temperatures higher than room temperature [1]. The II–VI alkaline-earth-metal oxides form a significant class of materials because they constitute a link between the highly ionic halides and the widely covalent semiconductors [15–17]. These compounds have attracted much attention due to their potential technological

✉ Habiba Lakhdari
habibalakhddari@gmail.com

✉ Bendouma Doumi
bdoummi@yahoo.fr

✉ Allel Mokaddem
mokaddem.allel@gmail.com

[1] Laboratory of Physico-Chemical Studies, University of Saida, 20000 Saida, Algeria

[2] Department of Physics, Faculty of Sciences, Dr. Tahar Moulay University of Saida, 20000 Saida, Algeria

[3] Centre Universitaire Nour Bachir El Bayadh, 32000 El Bayadh, Algeria

[4] Theoretical Physics Laboratory, U.S.T.H.B., Algiers, Algeria

[5] Unité de Catalyse et Chimie du Solide (UCCS), UMR CNRS 8181, Faculté des Sciences, Université d'Artois, Rue Jean Souvraz, SP 18, 62307 Lens, France

[6] IFIMUP and IN-Institute of Nanoscience and Nanotechnology, Universidade do Porto, 4169-007 Porto, Portugal

[7] Modelling and Simulation in Materials Science Laboratory, Physics Department, Djillali Liabes University of Sidi Bel-Abbes, 22000 Sidi Bel-Abbes, Algeria

applications ranging from catalysis to microelectronics [18–20].

The barium oxide (BaO) belongs to the II–VI alkaline-earth-metal binary oxides, which has a large band gap due to its high ionicity [18]; it is an important component for application of a thermionic electron emitter [21] Besides, the BaO is considered a potential DMS material in various applications for spintronics and optoelectronics, such as light emitting devices and ultralowpower memory devices [22–25] Recently, several studies have been carried out on the half-metallic and the magnetic properties in DMSbased II–VI such as the half-metallicity and magnetic properties of Cr-substituted BaTe [5], the half-metallic ferromagnetic behavior in $Sr_{1-x}V_xO$ [14], the half-metallic ferromagnets of Eu-doped alkaline-earth chalcogenides [26] the magnetic properties of $Zn_{1-x}TM_xTe$ (TM = Mn, Fe, Co, and Ni) [27], the magnetic characterization of nanocrystalline of $Zn_{1-x}Co_xO$ synthesized by combustion reaction [28], the magnetic properties of transition metaldoped II–VI oxide semiconductors [29] and the half-metallic ferromagnetism in vanadium-doped rock-salt SrO [30].

In this study, we have investigated the doping effect of chromium (Cr) impurity on the structural parameters, electronic structures and the half-metallic ferromagnetic properties of $Ba_{1-x}Cr_xO$ at various compositions x = 0.25, 0.5 and 0.75. We have used in our calculations the first-principle methods of density functional theory [31, 32] based on full-potential linearized augmented plane-wave approach within generalized gradient approximation functional of Wu and Cohen [33].

2 Methodology and Details of Calculations

The bulk BaO has conventional rock-salt NaCl (B1) structure with space group ($Fm\bar{3}m$) No. 225, which the Ba and O atoms are located respectively at the (0, 0, 0) and (0.5, 0.5, 0.5) sites. We have performed the $Ba_{1-x}Cr_xO$ supercells of eight atoms at concentrations x = 0.25, 0.5, and 0.75 by the substitution of one, two, and three Ba atoms by Cr impurities. For the concentration x = 0.5, we get the $Ba_{0.5}Cr_{0.5}O$ compound of tetragonal structure with space group of $P4/mmm$ No. 123. We have obtained for x = 0.25 and 0.75, respectively, the $Ba_{0.75}Cr_{0.25}O$ and $Ba_{0.25}Cr_{0.75}O$ compounds, which have cubic structures with space group of $Pm\bar{3}m$ No. 221 (see Fig. 1).

We have investigated the structural, electronic, and magnetic properties of $Ba_{0.75}Cr_{0.25}O$, $Ba_{0.5}Cr_{0.5}O$, and $Ba_{0.25}Cr_{0.75}O$ supercells by using the full-potential linearized augmented plane-wave (FP-LAPW) method as

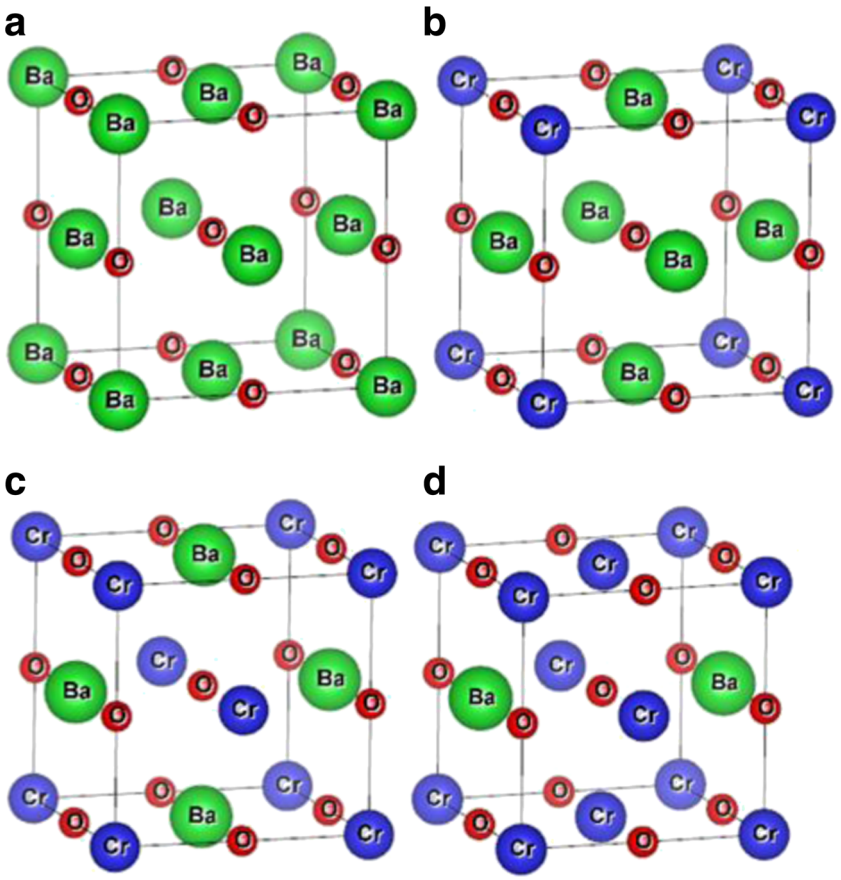

Fig. 1 Crystal structures of BaO and $Ba_{1-x}Cr_xO$ compounds at concentrations x = 0.25, 0.5, and 0.75. **a** BaO, **b** $Ba_{0.75}Cr_{0.25}O$, **c** $Ba_{0.5}Cr_{0.5}O$, and **d** $Ba_{0.25}Cr_{0.75}O$

Table 1 Calculated lattice constant (a), bulk modulus (B) and its pressure derivative (B') for BaO and $Ba_{1-x}Cr_xO$ at concentrations $x = 0.25$, 0.5 and 0.75

Compound	Concentration (x)	a (Å)	B (GPa)	B'	Method
This work					
BaO	0	5.507	78.59	4.91	GGA-WC
$Ba_{0.75}Cr_{0.25}O$	0.25	5.303	84.64	4.68	
$Ba_{0.5}Cr_{0.5}O$	0.5	5.056	98.64	4.65	
$Ba_{0.25}Cr_{0.75}O$	0.75	4.759	122.64	4.35	
Other calculations					
BaO	0	5.594 [18]			GGA-PBE
		5.58 [38]			GGA-PBE
		5.604 [39]	75 [39]	4.1 [39]	GGA-PBE
		5.478 [40]	82.36 [40]	4.21 [40]	LDA
		5.539 [41]	75.6 [43]	5.67 [44]	Experimental
		5.525 [42]			

implemented in WIEN2K code [34] based on density functional theory (DFT) [31, 32]. The exchange correlation potential is treated by the use of generalized gradient approximation functional of Wu and Cohen (GGA-WC) [33]. We have selected the average of the muffin-tin spheres radii of Ba, O, and Cr atoms in such a way that the muffin-tin spheres do not overlap. We have expanded the wave functions in the interstitial region to plane waves with a cutoff of $K_{max} = 9.0/R_{MT}$, where the R_{MT} is the average radius of the muffin-tin spheres and the K_{max} is the magnitude of the largest K vector in the plane wave. The charge density was Fourier expanded up to $G_{max} = 14$ (a.u.)$^{-1}$, where G_{max} is the largest vector in the Fourier expansion, whereas the maximum value for partial waves inside the atomic sphere was $l_{max} = 10$. We have used the cutoff of -6 Ry to determine the separation between the valence and the core states. For the Brillouin-zone integration, we have used the Monkhorst–Pack mesh [35, 36] of (4×4×3) k-points for $Ba_{0.5}Cr_{0.5}O$ and (4×4×4) k-points for BaO, $Ba_{0.75}Cr_{0.25}O$, and $Ba_{0.25}Cr_{0.75}O$. The self-consistent was achieved when the total energy convergence was set at 0.1 mRy.

3 Results and Discussions

3.1 Structural Properties

We have computed the structural parameters by the use of the empirical Murnaghan's equation of state [37] that describes the total energies as a function of equilibrium

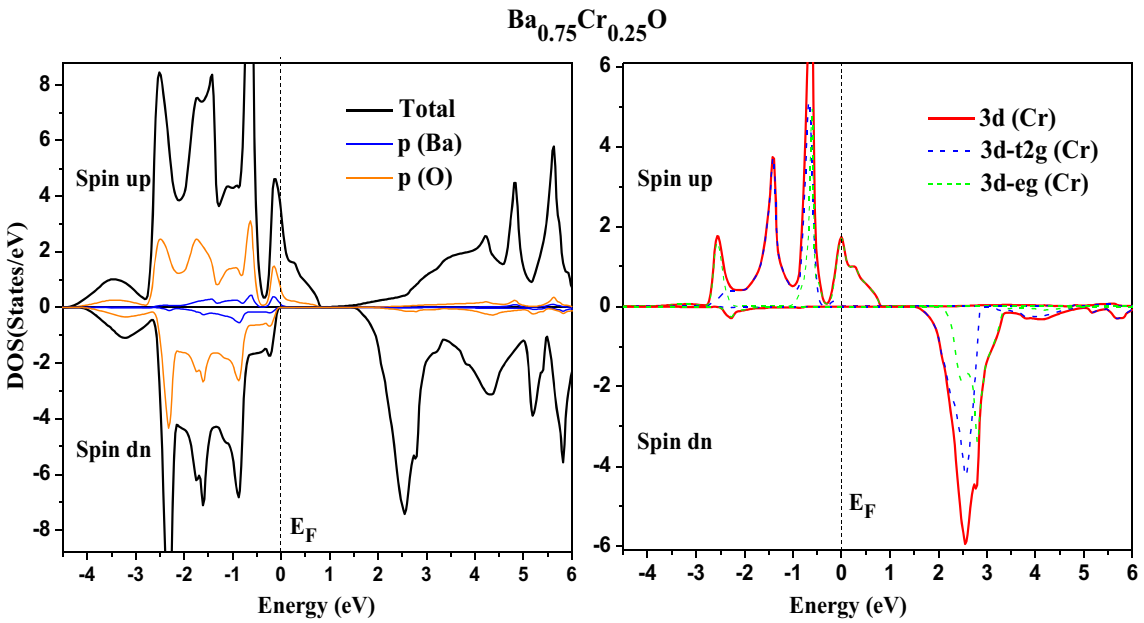

Fig. 2 Spin-polarized total and partial densities of states of $Ba_{0.75}Cr_{0.25}O$. The Fermi level is set to zero (*vertical dotted line*)

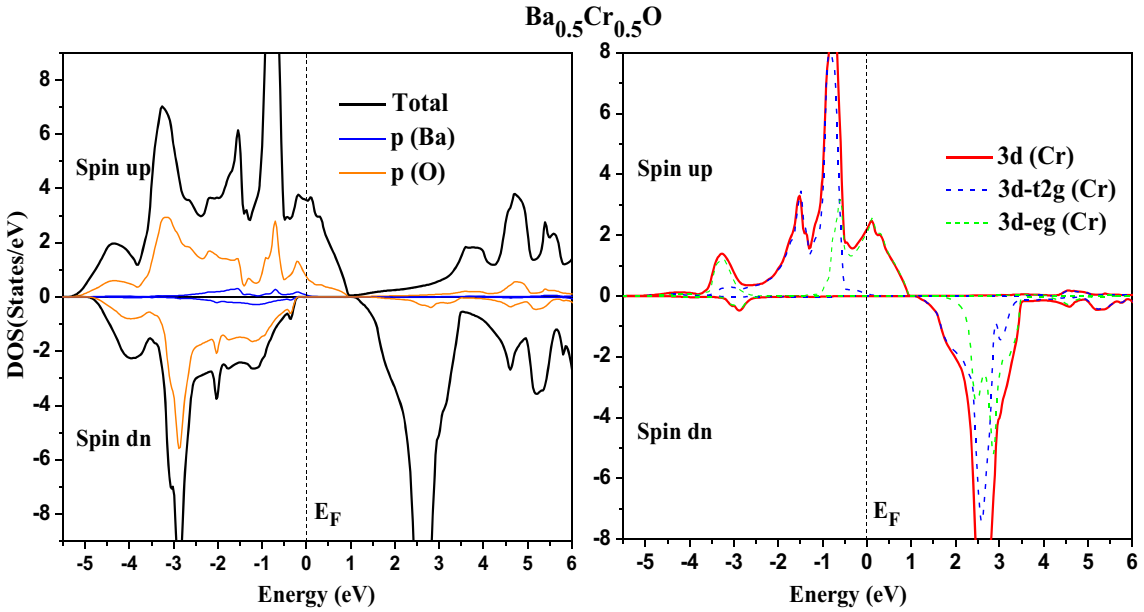

Fig. 3 Spin-polarized total and partial densities of states of $Ba_{0.5}Cr_{0.5}O$. The Fermi level is set to zero (*vertical dotted line*)

volumes. The obtained structural parameters such as the lattice constants (a), bulk modules (B), and its pressure derivatives (B') for the BaO and the $Ba_{1-x}Cr_xO$ at various concentrations, and other theoretical [18, 38–40] and experimental [41–44] results are summarized in Table 1. The lattice constant of BaO calculated with GGA-WC approach stay in good agreement with the experimental data [41–44], and it is better than the theoretical calculations of refs. [18, 38, 39] and ref. [40] found, respectively, by the generalized gradient approximation of Perdew-Burke-Ernzerhof (GGA-PBE) [45] and the local density approximation (LDA) [46]. This is due to the accurate performance of GGA-WC potential for determining the structural properties of solids [33, 47–52]. For $Ba_{1-x}Cr_xO$, we have found that the lattice parameter decreases with increasing concentration of Cr atom owing to a

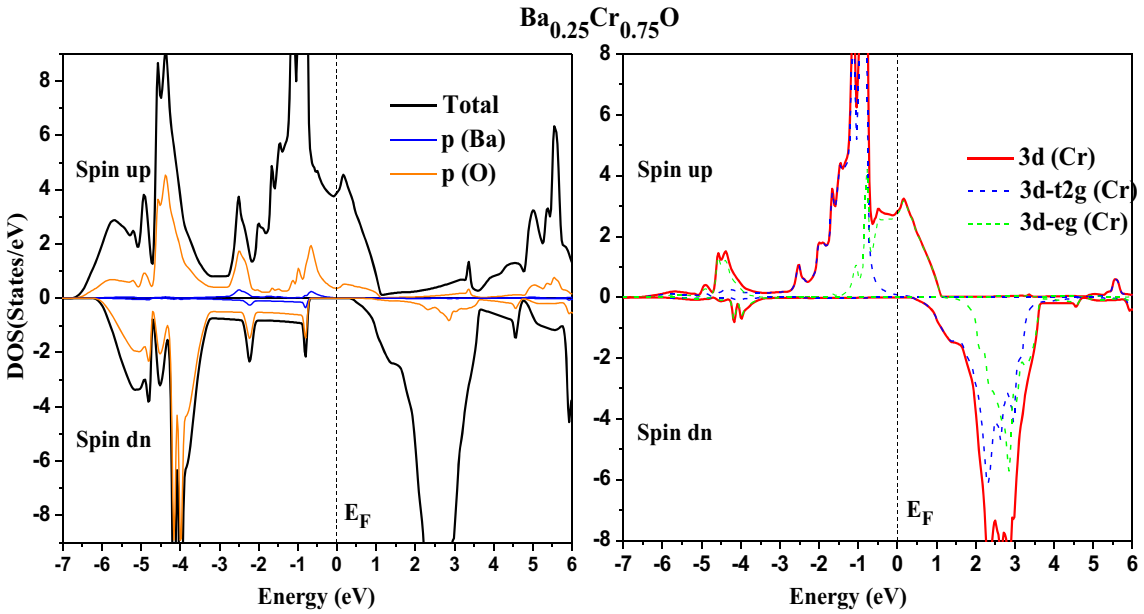

Fig. 4 Spin-polarized total and partial densities of states of $Ba_{0.25}Cr_{0.75}O$. The Fermi level is set to zero (*vertical dotted line*)

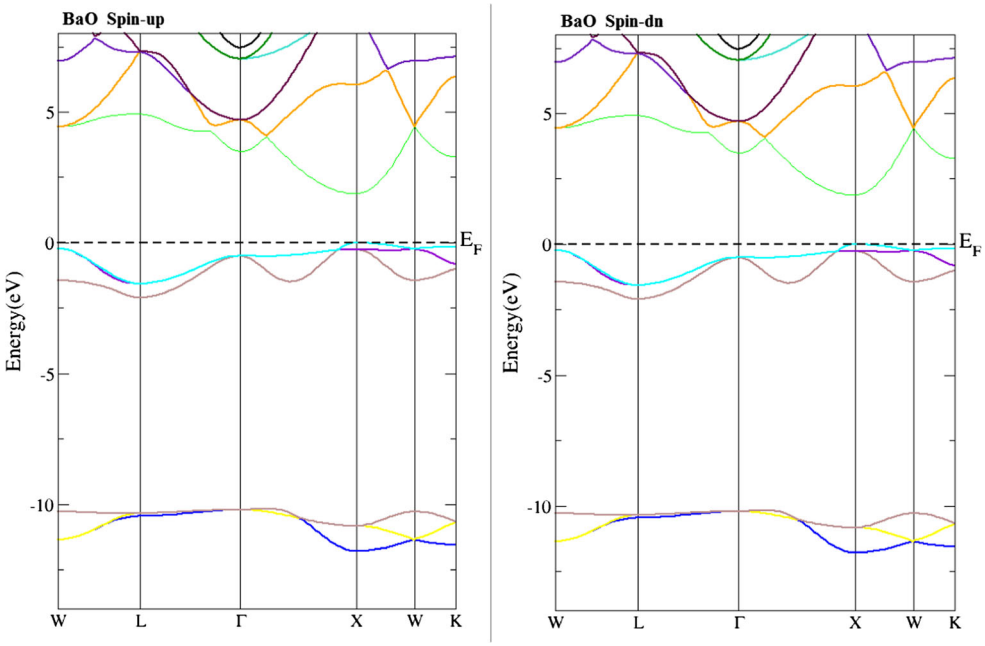

Fig. 5 Band structures of majority spin (*up*) and minority spin (*down*) for BaO. The Fermi level is set to zero (*horizontal dotted line*)

difference between Cr and Ba atomic radii. Consequently, the $Ba_{1-x}Cr_xO$ becomes harder when the concentration increases of Cr atom.

3.2 Electronic Structures and Half-Metallic Properties

In this section, we have used the calculated lattice parameters to describe the electronic and half-metallic properties of $Ba_{1-x}Cr_xO$ as a function of concentration x of chromium impurity. The projected partial and total densities of states (DOS) of $Ba_{0.75}Cr_{0.25}O$, $Ba_{0.5}Cr_{0.5}O$, and $Ba_{0.25}Cr_{0.75}O$ are given by Figs. 2, 3 and 4, respectively. To characterize the electronic structures of our compounds, we have investigated the DOS contribution around Fermi level (E_F) Figs. 2, 3 and 4 show that the majorityspin states are metallic whereas the gap occurs at E_F for the minority spin. The DOS of majority spin around E_F are mainly dominated by the contribution of hybridization between the 2p states of O atoms and 3d states of Cr impurities, while the DOS of minority spin are empty at E_F. Consequently, the $Ba_{1-x}Cr_xO$ compounds revealed a half-metallic feature at all concentrations Besides, the 3d (Cr) of majority-spin states are divided into levels the t_{2g} and e_g states,

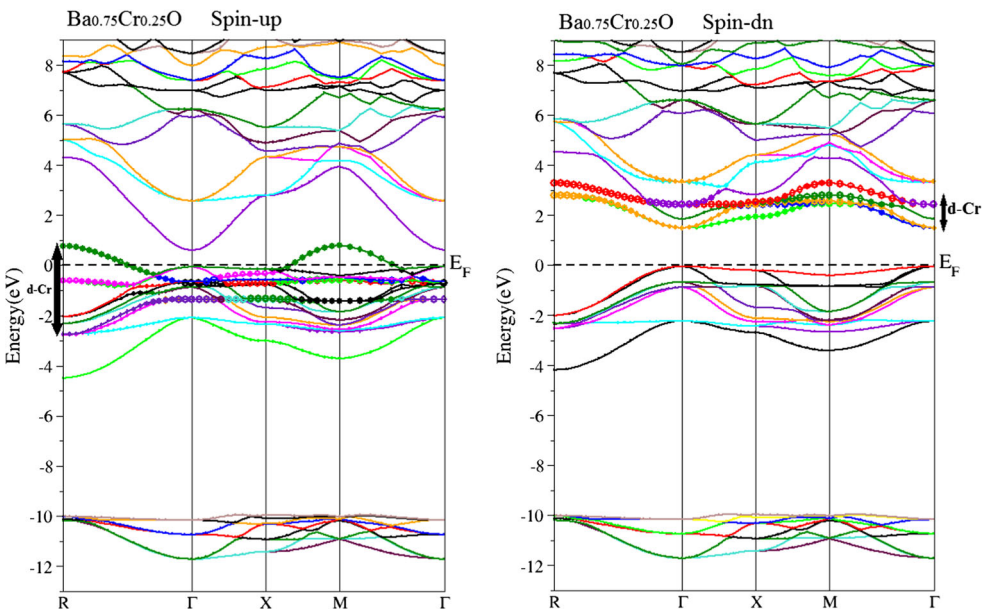

Fig. 6 Band structures of majority spin (*up*) and minority spin (*down*) for $Ba_{0.75}Cr_{0.25}O$, showing 3d (Cr) character bands by the filled-circle mode. The Fermi level is set to zero (*horizontal dotted line*)

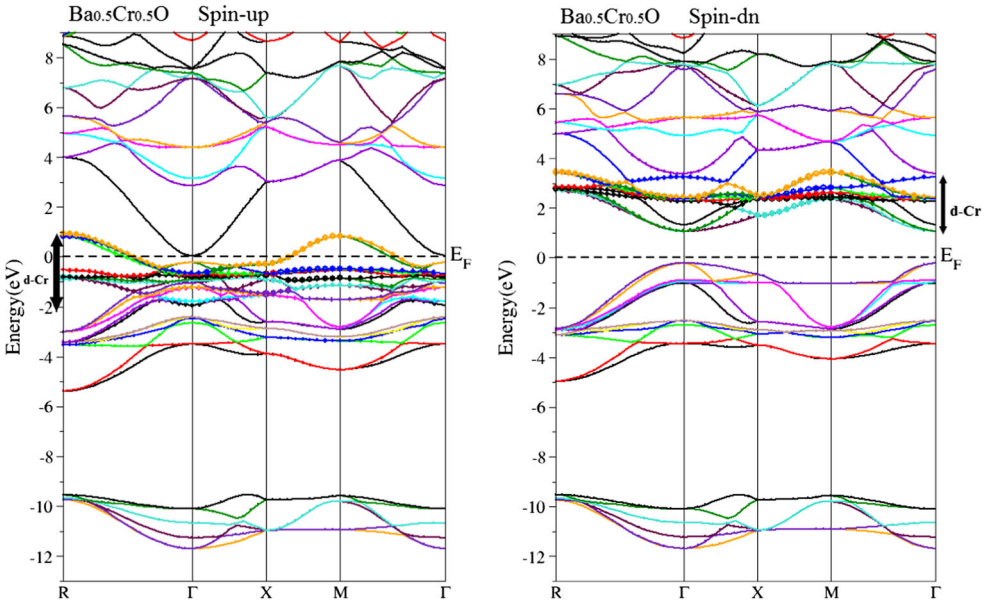

Fig. 7 Band structures of majority spin (*up*) and minority spin (*down*) for $Ba_{0.5}Cr_{0.5}O$, showing 3d (Cr) character bands by the filled-circle mode. The Fermi level is set to zero (*horizontal dotted line*)

which the t_{2g} are fully occupied and the e_g are partially occupied. Thus, the e_g states are located above t_{2g} states, indicating that the Cr impurity are located in the tetrahedral surroundings.

Figures 5, 6, 7 and 8 display the spin-polarized band structures of BaO, $Ba_{0.75}Cr_{0.25}O$, $Ba_{0.5}Cr_{0.5}O$ and $Ba_{0.25}Cr_{0.75}O$, respectively, where the 3d (Cr) bands are demonstrated by filled circles. The plots of doping systems depict that the majority-spin bands are characterized by the localized 3d (Cr) levels in the gap, while for minority-spin bands the completely empty 3d (Cr) levels are situated in conduction bands far than E_F Therefore, the majority-spin bands reveal a metallic character because some bands cut E_F whereas the minority-spin bands show forbidden bands around E_F Consequently, the spin-polarized band structures of $Ba_{1-x}Cr_xO$ are half-metallic ferromagnets with spin polarization of 100%.

Figure 5 shows clearly that the majority and minority spins of BaO have the same band structures with direct band gap (E^{XX}) located between the maximum valence bands and the minimum conduction bands at X high symmetry point On the other hand, Figs. 6, 7 and 8 show that majority-spin bands are more in number than minority spin bands owing to the exchange interaction between 2p (O) and 3d (Cr) levels, and hence the half-metallic ferromagnetic (HMF) gaps (G_{HMF}) and half-metallic gaps (G_{HM}) are

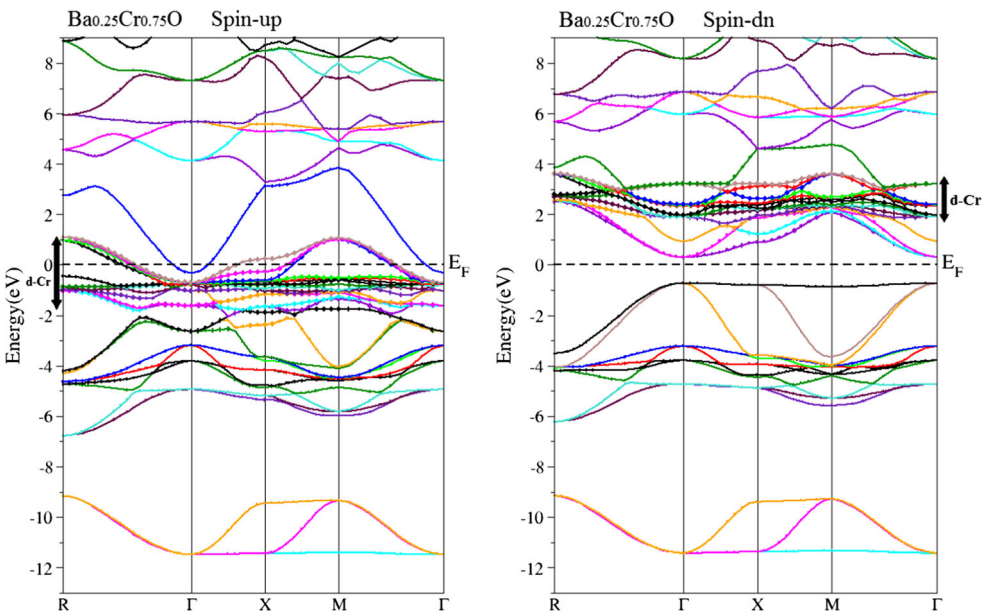

Fig. 8 Band structures of majority spin (*up*) and minority spin (*down*) for $Ba_{0.25}Cr_{0.75}O$, showing 3d (Cr) character bands by the filled-circle mode. The Fermi level is set to zero (*horizontal dotted line*)

Table 2 Calculated direct band gap E^{XX} for BaO, half-metallic ferromagnetic gap (G_{HMF}) and half-metallic gap (G_{HM}) of minority-spin bands for $Ba_{1-x}Cr_xO$ at concentrations $x = 0.25$, 0.5 and 0.75

Compound	Concentration (x)	G_{HMF} (eV)	G_{HM}(eV)	E^{XX} (eV)	Method	Behavior
This work						
BaO	0			1.884	GGA-WC	
$Ba_{0.75}Cr_{0.25}O$	0.25	1.549	0.055			HMF
$Ba_{0.5}Cr_{0.5}O$	0.5	1.277	0.218			HMF
$Ba_{0.25}Cr_{0.75}O$	0.75	1.032	0.308			HMF
Other calculations						
BaO	0			2.0 [18]	GGA-PBE	
				2.0 [53]	GGA-PBE	
				3.88 [54]	Experimental	
				4.1 [55]		
				3.985 [56]		

formed in the minority-spin bands. Our results of band gaps such as the direct band gap (E^{XX}) of BaO, and the HMF and HM gaps of minority-spin bands of $Ba_{1-x}Cr_xO$ at different concentrations with other theoretical [18, 53] and experimental [54–56] data are given in Table 2. The HM gap of a half-metallic material is defined as the minimum of the lowest energy of the majority (minority)-spin conduction bands with respect to the Fermi level and the absolute value of the highest energy of the majority (minority)-spin valence bands [57, 58]. The calculated direct band gap of 1.884 eV of BaO is in good agreement with the theoretical calculations of refs. [18, 53]. For $Ba_{1-x}Cr_xO$ compounds, we have found that $Ba_{0.75}Cr_{0.25}O$, $Ba_{0.5}Cr_{0.5}O$ and $Ba_{0.25}Cr_{0.75}O$ have direct HMF gaps of 1.549, 1.277 and 1.032 eV, respectively. From minority-spin bands, we understand that the 3d (Cr) bands broaden strongly in the gap with increasing concentration of Cr impurity, leading to the decrease of HMF gap The half-metallic gap is an important factor to determine the use of material in spintronics [50]; it is located between the minimum conduction bands and E_F for $Ba_{0.25}Cr_{0.75}O$ and between the maximum valence bands and E_F for both $Ba_{0.75}Cr_{0.25}O$ and $Ba_{0.5}Cr_{0.5}O$. The computed HM gap is 0.055 eV for $Ba_{0.75}Cr_{0.25}O$, 0.218 eV for $Ba_{0.5}Cr_{0.5}O$ and 0.308 eV for $Ba_{0.25}Cr_{0.75}O$, which increases with increasing of Cr concentration. The $Ba_{1-x}Cr_xO$ compounds are half-metallic ferromagnetic with HM gaps which make them potential materials for possible spintronics applications.

3.3 Magnetic Properties

The magnetism in the $Ba_{1-x}Cr_xO$ doping systems is induced by the 3d states of magnetic Cr impurity, which is partially filled with four electrons. According to the Hund's rule, these unpaired electrons create a total magnetic moment of 4 Bohr magneton (μ_B) per Cr atom in $Ba_{1-x}Cr_xO$ materials. Table 3 summarizes the calculated total magnetic moment (MM), local MM for Cr, Ba, and O atoms, and MM in the interstitial site per Cr atom for $Ba_{0.75}Cr_{0.25}O$, $Ba_{0.5}Cr_{0.5}O$, and $Ba_{0.25}Cr_{0.75}O$. The partial MM of the Cr atom for each compound is less than 4 μ_B, and minor magnetic moments are induced in the Ba, O, and interstitial sites; this is due to the p–d exchange interaction between the 2p (O) and 3d (Cr) states. For all compounds, the magnetic moments of Cr and O atoms are antiparallel, implying that the valence bands interact anti-ferromagnetically with Cr magnetic spins. The positive magnetic spins of Cr and Ba atoms for $Ba_{0.75}Cr_{0.25}O$ and $Ba_{0.5}Cr_{0.5}O$ depict the ferromagnetic interaction between Cr and Ba sites, while the opposite sign of magnetic moments of Cr and Ba atoms for $Ba_{0.25}Cr_{0.75}O$ describes the anti-ferromagnetic interaction between Cr and Ba sites.

We have employed the results of the electronic band structures to calculate the exchange coupling between magnetic impurity and valence (conduction) bands such as the s–d exchange constants $N_0\alpha$ (conduction band) and the p–d exchange constants $N_0\beta$ (valence band). These

Table 3 Calculated total and local magnetic moments per Cr atom (in Bohr magneton (μ_B)) within the muffin-tin spheres and in the interstitial sites for $Ba_{1-x}Cr_xO$ at concentrations $x = 0.25$, 0.5 and 0.75

Compound	Concentration (x)	Total (μ_B)	Cr (μ_B)	Ba (μ_B)	O (μ_B)	Interstitial (μ_B)
$Ba_{0.75}Cr_{0.25}O$	0.25	4	3.841	0.013	− 0.243	0.391
$Ba_{0.5}Cr_{0.5}O$	0.5	4	3.707	0.008	− 0.167	0.457
$Ba_{0.25}Cr_{0.75}O$	0.75	4	3.489	− 0.004	− 0.058	0.574

Table 4 Calculated p–d exchange splitting $\Delta_x^v(pd) = E_v^{\downarrow} - E_v^{\uparrow}$ and $\Delta_x^c(pd) = E_c^{\downarrow} - E_c^{\uparrow}$ and exchange constants $N_0\alpha$ and $N_0\beta$ for $Ba_{1-x}Cr_xO$ at concentrations $x = 0.25$, 0.5, and 0.75

Compound	Concentration (x)	$\Delta_x^c(pd)$ (eV)	$\Delta_x^v(pd)$ (eV)	$N_0\alpha$	$N_0\beta$
$Ba_{0.75}Cr_{0.25}O$	0.25	0.906	0.005	1.812	0.010
$Ba_{0.5}Cr_{0.5}O$	0.5	1.016	0.002	1.016	0.002
$Ba_{0.25}Cr_{0.75}O$	0.75	0.633	− 0.024	0.422	− 0.016

two important parameters are determined from mean-field theory by the following expressions [59, 60]:

$$N_0\alpha = \frac{\Delta E_c}{x\langle s\rangle} \tag{1}$$

$$N_0\beta = \frac{\Delta E_v}{x\langle s\rangle} \tag{2}$$

where the $\Delta E_c = E_c^{\downarrow} - E_c^{\uparrow}$ is the conduction band-edge spin splittings and the $\Delta E_v = E_v^{\downarrow} - E_v^{\uparrow}$ is the valence band-edge spin splittings of $Ba_{1-x}Cr_xO$ at Γ high symmetry point. The $\langle s\rangle$ is the half total magnetic moment per Cr atom [59], and the $x$is the concentration of Cr atom. Moreover we have described the attraction character in the $Ba_{1-x}Cr_xO$ doping materials by determining the two important p–d exchange splitting $\Delta_x^v(pd) = E_v^{\downarrow} - E_v^{\uparrow}$ and $\Delta_x^c(pd) = E_c^{\downarrow} - E_c^{\uparrow}$.

Our results of $N_0\alpha$ and $N_0\beta$ exchange constants and $\Delta_x^v(pd)$ and $\Delta_x^c(pd)$ p–d exchange splittings are given in Table 4 The positive sign of $N_0\alpha$ and $N_0\beta$, respectively at the concentrations ($x = 0.25$, 0.5 and 0.75) and ($x = 0.25$ and 0.5), describes the ferromagnetic coupling between 3d (Cr) states and valence (conduction) bands. In contrast, the coupling is anti-ferromagnetic between 3d (Cr) states and valence bands in the case of negative value of $N_0\beta$ for the concentration $x = 0.75$. On the other hand, the results of p–d exchange splitting show the negative value of $\Delta_x^v(pd)$ for $Ba_{1-x}Cr_xO$ at concentration $x = 0.75$, revealing that the potential of minority spin is effective with respect to the majority spin [61], which is an important feature for the spin-polarized compounds [61, 62].

4 Conclusion

We have employed the DFT first-principle methods with FP-LAPW approach and GGA-WC exchange potential to investigate the effect of Cr impurity on the structural, electronic, and ferromagnetic properties of $Ba_{1-x}Cr_xO$ at various concentrations $x = 0.25$, 0.5, and 0.75. The optimized structural parameters show that the lattice constant of $Ba_{1-x}Cr_xO$ doping compound decreases with increasing concentration of Cr impurity compared with binary BaO; this is due to the difference between Cr and Ba atomic radii. The total magnetic moments of 4 μ_B and the ferromagnetic coupling between host valence bands and the 3d (Cr) states confirm the magnetic character of $Ba_{1-x}Cr_xO$ materials. From our findings of electronic and magnetic properties, we have predicted that the $Ba_{1-x}Cr_xO$ compounds are half-metallic ferromagnetic with half-metallic gaps and spin polarization of 100%, which make them promising candidates for possible spintronics applications.

References

1. Akbar, W., Nazir, S.: Origin of p-type half-metallic ferromagnetism in carbon-doped BeS: first-principles characterization. Alloy. Compd. **743**, 83–86 (2018)
2. Lone, I.U.N., Sirajuddeen, M.M.S.: Half metallic ferromagnetism in gallium and zinc doped chromium phosphide: first principles calculations. Mater. Chem. Phys. **203**, 65–72 (2018)
3. Movlarooy, T.: J. Magn. Magn. Mater. **441**, 139–148 (2017)
4. Espitia-Rico, M.J., Parra, O.S., López, C.O.: Electronic and magnetic behavior of transition metal-doped cubic gallium nitride: first-principles calculations. J. Magn. Magn. Mater. **451**, 295–299 (2018)
5. Berriah, K., Doumi, B., Mokaddem, A., Elkeurti, M., Sayede, A., Tadjer, A., Araújo, J.P.: Theoretical investigation of electronic performance, half-metallicity, and magnetic properties of Cr-substituted BaTe. J. Comput. Electron. **17**, 909–919 (2018)
6. Doumi, B., Mokaddem, A., Ishak-Boushaki, M., Bensaid, D.: First-principle investigation of magnetic and electronic properties of vanadium- and chromium-doped cubic aluminum phosphide. Sci. Semicond. Process. **32**, 166–171 (2015)
7. Doumi, B., Mokaddem, A., Sayede, A., Dahmane, F., Mogulkoc, Y., Tadjer, A.: First-principles investigations on ferromagnetic behaviour of $Be_{1-x}V_xZ$ (Z = S, Se and Te) ($x = 0.25$). Superlattice. Microstruct. **88**, 139–149 (2015)
8. Zhang, L., Wang, X., Cheng, Z.: Electronic, magnetic, mechanical, half-metallic and highly dispersive zero-gap half-metallic properties of rare-earth-element-based quaternary Heusler compounds. Alloy. Compd. **718**, 63–74 (2017)
9. Yu, Y.B., Thompson, S.M.: Spintronic materials and technology. Taylor & Francis Group, New York (2006)
10. Kaminska, M., Twardowski, A., Wasik, D.: Mn and other magnetic impurities in GaN and other III–v semiconductors-perspective for spintronic applications. J. Mater. Sci.: Mater. Electron. **19**, 828–834 (2008)
11. Liu, J., Kang, W., Yang, X.L., Ma, C.G., Zheng, R.L.: Electronic structures of several new rare-earth half-metallic ferromagnets SmX (X = O, S, Se, and Te). J. Supercond. Nov. Magn. **31**, 1227–1233 (2018)

12. Doumi, B., Tadjer, A., Dahmane, F., Djedid, A., Yakoubi, A., Barkat, Y., Ould Kada, M., Sayede, A., Hamada, L.: First-principles investigation of half-metallic ferromagnetism in V-doped BeS, BeSe, and BeTe. J. Supercond. Nov. Magn. **27**, 293–300 (2014)
13. Doumi, B., Mokaddem, A., Temimi, L., Beldjoudi, N., Elkeurti, M., Dahmane, F., Sayede, A., Tadjer, A., Ishak-Boushaki, M.: First-principle investigation of half-metallic ferromagnetism in octahedrally bonded Cr-doped rock-salt SrS, SrSe, and SrTe. Eur. Phys. J. B **88**, 93 (2015)
14. Berber, M., Doumi, B., Mokaddem, A., Mogulkoc, Y., Sayede, A., Tadjer, A.: Investigation of electronic structure and half-metallic ferromagnetic behavior with large half-metallic gap in $Sr_{1-x}V_xO$. J. Comput. Electron. **16**, 542–547 (2017)
15. Alfredsson, M., Brodholt, J.P., Wilson, P.B., Price, G.D., Cora, F., Calleja, M., Bruin, R., Blanshard, L.J., Tyers, R.P.: Structural and magnetic phase transitions in simple oxides using hybrid functional. Mol. Simulat. **31**, 367 (2005)
16. Bhardwaj, P., Singh, S., Gaur, N.K.: Structural, elastic and thermophysical properties of divalent metal oxides with NaCl structure. Mater. Res. Bull. **44**, 1366–1374 (2009)
17. Bhardwaj, P., Singh, S.: Pressure induced structural phase transitions–A review. Cent. Eur. J. Chem. **10**, 1391–1422 (2012)
18. Yang, X., Wang, Y., Yan, H., Chen, Y.: Effects of epitaxial strains on spontaneous polarizations and band gaps of alkaline-earth-metal oxides MO (M = Mg, Ca, Sr, Ba). Comp. Mater. Sci. **121**, 61–66 (2016)
19. Schütt, O., Pavone, P., Windl, W., Karch, K., Strauch, D.: Ab initio lattice dynamics and charge fluctuations in alkaline-earth oxides. Phys. Rev. B **50**, 3746 (1994)
20. Oganov, A.R., Dorogokupets, P.I.: All-electron and pseudopotential study of MgO: equation of state, anharmonicity, and stability. Phys. Rev. B **67**, 224110 (2003)
21. Khatib, M., Korek, M.: Electronic structure of the BaO molecule with dipole moments and ro-vibrational calculations. Spectrochim. Acta A **192**, 401–410 (2018)
22. Kenmochi, K., Ann Dinh, V., Sato, K., Yanase, A., Katayama-Yoshida, H.: Materials design of transparent and half-metallic ferromagnets of MgO, SrO and BaO without magnetic elements. J. Phys. Soc. Jpn. **73**, 2952 (2004)
23. Kemmochi, K., Seike, M., Sato, K., Yanase, A., Katayama-Yoshida, H.: New class of high-T C diluted ferromagnetic semiconductors based on CaO without transition metal elements. J. Supercond. **18**, 37–40 (2005)
24. Katayama-Yoshida, H., Sato, K., Fukushima, T., Toyoda, M., Kizaki, H., Dinh, V.A., Dederichs, P.H.: Theory of ferromagnetic semiconductors. Phys. Stat. Sol. **204**, 15–32 (2007)
25. Albanese, E., Pacchioni, G.: Ferromagnetism in nitrogen doped BaO: a self interaction corrected DFT study. Phys. Chem. Chem. Phys. **19**, 3279–3286 (2017)
26. Jun, L., Xiao-Lan, Y., Wei, K.: Research on new rare-earth half-metallic ferromagnets $X_{0.75}Eu_{0.25}O$ (X = Ca, Sr and Ba) based on the first-principles calculations. Solid State Commun. **242**, 11–15 (2016)
27. Mahmood, Q., Hassan, M., Faridi, M.A.: Study of magnetic and optical properties of $Zn_{1-x}TM_xTe$ (TM = Mn, Fe, Co, Ni) diluted magnetic semiconductors: first principle approach. Chin. Phys. B **26**, 027503 (2017)
28. Torquato, R.A., Shirsath, S.E., Kiminami, R.H.G.A., Costa, A.C.F.M.: Synthesis and structural, magnetic characterization of nanocrystalline $Zn_{1-x}Co_xO$ diluted magnetic semiconductors (DMS) synthesized by combustion reaction. Ceram. Int. **44**, 4126–4131 (2018)
29. Shahjahan, M., Nizu, S.Y.: Numerical study of magnetic states and magnetic properties of transition metal doped II-VI oxide semiconductors. Comput. Condens. Matter **16**, e00305 (2018)
30. Berber, M., Doumi, B., Mokaddem, A., Mogulkoc, Y., Sayede, A., Tadjer, A.: First-principle predictions of electronic properties and half-metallic ferromagnetism in vanadium-doped rock-salt SrO. J. Electron. Mater. **47**, 449–456 (2018)
31. Hohenberg, P., Kohn, W.: Inhomogeneous electron gas. Phys. Rev. **136**, B864–871 (1964)
32. Kohn, W., Sham, L.J.: Self-consistent equations including exchange and correlation effects. Phys. Rev. **140**, A1133–1138 (1965)
33. Wu, Z., Cohen, R.E.: More accurate generalized gradient approximation for solids. Phys. Rev. B **73**, 235116 (2006)
34. Blaha, P., Schwarz, K., Madsen, G.K.H., Kvasnicka, D., Luitz, J.: WIEN2K, an Augmented Plane Wave plus Local Orbitals Program for Calculating Crystal Properties. Vienna University of Technology, Vienna (2001)
35. Monkhorst, H.J., Pack, J.D.: Special points for Brillonin-zone integrations. Phys. Rev. B **13**, 5188–5192 (1976)
36. Pack, J.D., Monkhorst, H.J.: Special points for Brillouin-zone integrations"–a reply. Phys. Rev. B **16**, 1748–1749 (1977)
37. Muranghan, F.D.: The compressibility of media under extreme pressures. Proc. Natl. Acad. Sci. U.S.A. **30**, 244–247 (1944)
38. Nejatipour, H., Dadsetani, M.: Excitonic effects in the optical properties of alkaline earth chalcogenides from first-principles calculations. Phys. Scr. **90**, 085802 (2015)
39. Cinthia, A.J., Priyanga, G.S., Rajeswarapalanichamy, R., Iyakutti, K.: Structural, electronic and mechanical properties of alkaline earth metal oxides MO (M = Be, Mg, Ca, Sr, Ba). J. Phys. Chem. Solids **79**, 23–42 (2015)
40. Santana, J.A., Krogel, J.T., Kent, P.R., Reboredo, F.A.: Cohesive energy and structural parameters of binary oxides of groups IIA and IIIB from diffusion quantum Monte Carlo. J. Chem. Phys. **144**, 174707 (2016)
41. Liu, L.G., Bassett, W.A.: Effect of pressure on the crystal structure and the lattice parameters of BaO. J. Geophys. Res. **77**, 4934–4937 (1972)
42. Kaneko, Y., Morimoto, K., Koda, T.: Optical properties of alkaline-earth chalcogenides. I. Single crystal growth and infrared reflection spectra due to optical phonons. J. Phys. Soc. Jpn. **51**, 2247–2254 (1982)
43. PARK, K.O., Sivertsen, J.M.: Temperature dependence of the bulk modulus of BaO single crystals. J. Am. Ceram. Soc. **60**, 537 (1977)
44. Chang, Z.P., Graham, E.K.: Elastic properties of oxides in the NaCl-structure. J. Phys. Chem. Solids **38**, 1355–1362 (1977)
45. Perdew, J.P., Burke, K., Ernzerhof, M.: Generalized gradient approximation made simple. Phys. Rev. Lett. **77**, 3865 (1996)
46. Perdew, J.P., Zunger, A.: Self-interaction correction to density-functional approximations for many-electron systems. Phys. Rev. B **23**, 5048 (1981)
47. Sharma, S., Verma, A.S., Bhandari, R., Kumari, S., Jindal, V.K.: First principles study of the structural, electronic, optical, elastic and thermodynamic properties of $CdXAs_2$ (X=Si, Ge and Sn). Mater. Sci. Semicond. Process **27**, 79–96 (2014)
48. Sajjad, M., Manzoor, S., Zhang, H.X., Noor, N.A., Alay-e-Abbas, S.M., Shaukat, A., Khenata, R.: The half-metallic ferromagnetism character in $Be_{1-x}V_xY$ (Y = Se and Te) alloys: an ab-initio study. J. Magn. Magn. Mater. **379**, 63–73 (2015)
49. Doumi, B., Mokaddem, A., Sayede, A., Boutaleb, M., Tadjer, A., Dahmane, F.: Half-metallic ferromagnetic property related to spintronic applications in 3d (V, Cr, and Mn)-doped GaP DMSs. J. Supercond. Novel Magn. **28**, 3163 (2015)

50. Doumi, B., Mokaddem, A., Dahmane, F., Sayede, A., Tadjer, A.: A novel theoretical design of electronic structure and half-metallic ferromagnetism in the 3d (V)-doped rock-salts SrS, SrSe, and SrTe for spintronics. RSC Adv. **112**, 92328 (2015)
51. Addadi, Z., Doumi, B., Mokaddem, A., Elkeurti, M., Sayede, A., Tadjer, A., Dahmane, F.: Electronic and ferromagnetic properties of 3d(V)-doped (BaS) barium sulfide. J. Supercond. Nov. Magn. **30**, 917–923 (2017)
52. Zerouali, A., Mokaddem, A., Doumi, B., Dahmane, F., Elkeurti, M., Sayede, A., Tadjer, A.: First-principle calculations of electronic and ferromagnetic properties of $Al_{1-x}V_xSb$. J. Comput. Electron. **15**, 1255–1262 (2016)
53. McLeod, J.A., Wilks, R.G., Skorikov, N.A., Finkelstein, L.D., Abu-Samak, M., Kurmaev, E.Z., Moewes, A.: Band gaps and electronic structure of alkaline-earth and post-transition-metal oxides. Phys. Rev. B **81**, 245123 (2010)
54. Zolweg, R.J.: Optical absorption and photoemission of barium and strontium oxides, sulfides, selenides, and tellurides. Phys. Rev. **111**, 113–119 (1958)
55. Saum, G.A., Hensley, E.B.: Fundamental optical absorption in the IIA-VIB compounds. Phys. Rev. **113**, 1019–1022 (1959)
56. Kaneko, Y., Koda, T.: New developments in IIa–VIb (alkaline-earth chalcogenide) binary semiconductors. J. Cryst. Growth **86**, 72–78 (1988)
57. Yao, K.L., Gao, G.Y., Liu, Z.L., Zhu, L.: Half-metallic ferromagnetism of zinc-blende CrS and CrP: a first-principles pseudopotential study. Solid State Commun. **133**, 301 (2005)
58. Gao, G.Y., Yao, K.L., Şaşoğlu, E., Sandratskii, L.M., Liu, Z.L., Jiang, J.L.: Half-metallic ferromagnetism in zinc-blende CaC, SrC, and BaC from first principles. Phys. Rev. B **75**, 174442 (2007)
59. Sanvito, S., Ordejon, P., Hill, N.A.: First-principles study of the origin and nature of ferromagnetism in $Ga_{1-x}Mn_xAs$. Phys. Rev. B **63**, 165206 (2001)
60. Raebiger, H., Ayuela, A., Nieminen, R.M.: Intrinsic hole localization mechanism in magnetic semiconductors. J. Phys. Condens. Matter **16**, L457 (2004)
61. Verma, U.P., Sharma, S., Devi, N., Bisht, P.S., Rajaram, P.: Spin-polarized structural, electronic and magnetic properties of diluted magnetic semiconductors $Cd_{1-x}Mn_xTe$ in zinc blende phase. J. Magn. Magn. Mater. **323**, 394–399 (2011)
62. Morozzi, V.L., Janak, J.F., Williams, A.R.: Calculated Electronic Properties of Metals. Pergamon, New York (1978)